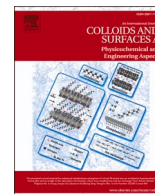




Contents lists available at ScienceDirect

Colloids and Surfaces A: Physicochemical and Engineering Aspects

journal homepage: www.elsevier.com/locate/colsurfa

Adsorption of rare earth elements (Ce^{3+} , La^{3+} , and Nd^{3+}) and recovery from phosphogypsum leachate using a novel ZSM-5 zeolite

Guilherme Luiz Dotto^a, Diana Pinto^b, Luis Felipe Oliveira Silva^{b,*}, Alejandro Grimm^c, Mohammad Rizwan Khan^d, Naushad Ahmad^d, Irineu A.S. de Brum^e, Jyri-Pekka Mikkola^{f,g}, Glaydson S. dos Reis^{c,*}

^a Research Group on Adsorptive and Catalytic Process Engineering (ENGEPA), Federal University of Santa Maria, Av. Roraima, 1000-7, Santa Maria, RS 97105-900, Brazil

^b Universidad De La Costa, Calle 58 # 55-66, Barranquilla, Atlántico 080002, Colombia

^c Department of Forest Biomaterials and Technology, Biomass Technology Centre, Swedish University of Agricultural Sciences, Umeå SE-901 83, Sweden

^d Department of Chemistry, College of Science, King Saud University, Riyadh 11451, Saudi Arabia

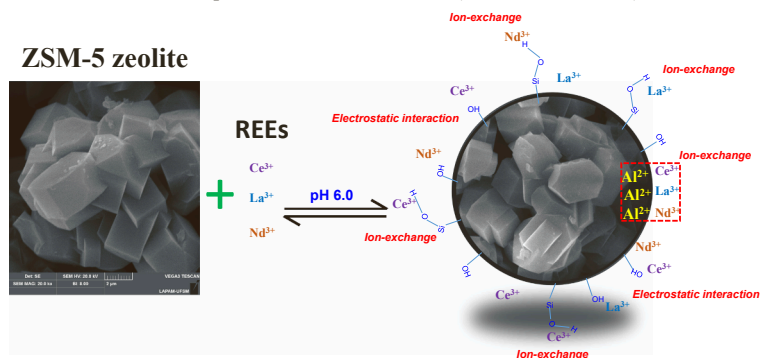
^e Mineral Processing Laboratory, Federal University of Rio Grande do Sul, 9500 Bento Gonçalves Avenue, Porto Alegre 91501-970, Brazil

^f Technical Chemistry, Department of Chemistry, Chemical-Biological Center, Umeå University, Umeå 90187, Sweden

^g Industrial Chemistry and Reaction Engineering, Johan Gadolin Process Chemistry Centre, Åbo Akademi University, Åbo-Turku 20500, Finland

GRAPHICAL ABSTRACT

Adsorption of rare earth elements (Ce^{3+} , La^{3+} , and Nd^{3+})



ARTICLE INFO

Keywords:

Microporous zeolite
Adsorption of rare earth elements
Ion-exchange mechanism

ABSTRACT

ZSM-5 zeolite is a multifunctional material highly efficient for adsorbing ions. Our ZSM-5 was synthesized by employing a nucleating gel as a structure-directing agent, followed by homogenization and hydrothermal treatment. The as-prepared ZSM-5 was physicochemically characterized to assess its properties. Next, the as-prepared zeolite was employed as an adsorbent to remove rare earth elements, REEs from synthetic solutions and real phosphogypsum leachate under batch mode operation. As expected, the ZSM-5 adsorbent was discovered to be highly microporous with abundant surface functionalities, which could positively impact REE adsorption. The adsorption data indicated a high affinity between ZSM-5 and all three REEs with rapid kinetics

* Corresponding authors.

E-mail addresses: glaydson.simoes.dos.reis@slu.se (L.F.O. Silva), glaydson.simoes.dos.reis@slu.se (G.S. dos Reis).

<https://doi.org/10.1016/j.colsurfa.2024.134549>

Received 12 May 2024; Received in revised form 13 June 2024; Accepted 17 June 2024

Available online 17 June 2024

0927-7757/© 2024 The Author(s). Published by Elsevier B.V. This is an open access article under the CC BY license (<http://creativecommons.org/licenses/by/4.0/>).

and high adsorption capacities. The modeling study suggested that the adsorption kinetic data were well fitted by Avrami-fractional order, and Liu described the equilibrium data. The maximum adsorption capacity for Ce^{3+} , La^{3+} , and Nd^{3+} were 99.42 mg g^{-1} , 96.43 mg g^{-1} , 118.10 mg g^{-1} , respectively. Further, the thermodynamic analysis revealed that the interaction between ZSM-5 and Ce^{3+} , La^{3+} , and Nd^{3+} was favorable, spontaneous, and endothermic. The efficiency of ZSM-5 adsorbent was also studied in recovering several REEs from leachate of phosphogypsum wastes, and the data results proved its potency to do so. The findings reported in this work support the idea that ZSM-5 can be successfully used as an adsorbent to recover REEs from synthetic and real samples.

1. Introduction

Rare earth elements (REEs) are essential for a wide range of modern technologies, including electric vehicles, wind turbines, smartphones, and medical devices. The global supply of REEs is dominated by a few countries, among which China is the largest producer, with more than 80 % of the world's market [1,2]. This concentrated supply could be used to exert economic pressure on other countries, restrict access to critical technologies, or lead to concerns about REEs scarcity and its impact on industries that rely on these. Mining and processing of these elements also come along with significant environmental impacts, including water pollution, air pollution, and land degradation [2,3]. The problems related to REEs scarcity are complex, and there is no easy solution. However, by taking steps to develop new sources of REEs, reduce demand, and recycle, the risks associated with REEs scarcity can be mitigated [4,5].

The recovery of REEs from secondary sources is becoming increasingly important as the demand for these elements grows [6,7]. These sources offer several advantages over primary sources, such as an environmentally friendly approach, less energy expenditure, lower CO_2 footprint, wide worldwide availability, easier extraction, and so forth [8]. The recovery of REEs from secondary sources is still in its early stages, but it is a promising area of research. As the demand for REEs continues to grow, this technology is likely to become increasingly important [4]. Secondary sources of REEs are those that are not mined from the earth but are recovered from waste products or recycled materials. These sources include materials such as slags from the refining of metals [9], bauxite residue (red mud) from the aluminum industry [10], mine tailings [11], electronic waste [12], and phosphogypsum [13–16]. The latter is a by-product of the wet process of phosphoric acid and fertilizer production based on phosphate rock [6]. The concentration of REEs in phosphogypsum varies depending on the source of the phosphate rock [6,17]. According to Walawalkar et al. [17], the contents of REEs in phosphogypsum (from Kapuskasing phosphate rock) are in the range of $1\text{--}53 \text{ mg kg}^{-1}$. The authors found that the most abundant REEs are yttrium (Y), lanthanum (La), cerium (Ce), neodymium (Nd), samarium (Sm), gadolinium (Gd) and praseodymium (Pr).

The extraction of REEs from phosphogypsum is a relatively new process. There are several different methods for extracting REEs from phosphogypsum, usually including a combination of processes such as acid leaching [13], solvent extraction, and adsorption [15–18]. Adsorption shows up to be one of the most suitable and efficient methods due to its simpler operation and high effectiveness in removing ions from water media, and it presents the advantage of employing a wide range of low-cost and sustainable adsorbents [14–17]. Among these adsorbents, zeolites have been widely used as potent adsorbents for the separation process since their industrial breakthrough in the 1950s and continue to be employed in many separations (and other industrial) processes [18,19]. Zeolites are a type of porous crystalline materials that have a high surface area and a negatively charged framework that create an ion-exchange ability that renders them well-suited for the adsorption of cations, such as rare earth elements (REEs).

Zeolites occur naturally in abundance as well as they can be prepared in the laboratory [17,18]. Synthetic zeolites have attracted enormous

interest from the research community due to their easy and scalable preparation methods and easy control of their physicochemical properties, such as pore structure and surface functionalities [17,18]. Synthetic zeolites may also offer the advantage of having a larger pore volume than natural zeolites, which favors their uses as adsorbents for adsorbing/trapping various contaminants (molecules and ions) from wastewater [17,18].

In this work, a zeolite material (ZSM-5) with adjusted microporosity and high presence of surface functionalities was synthesized and employed as an effective adsorbent for the adsorption and recovery of cerium (Ce^{3+}), lanthanum (La^{3+}), and neodymium (Nd^{3+}) from synthetic and real samples. The as-prepared zeolite was characterized using analytical techniques such as FT-IR, XRD, SEM, TGA, and BET analysis. The adsorption process was characterized by measuring the effect of the pH of the solution on the adsorption capacity, kinetic, isotherm, and thermodynamics of adsorption. To study the potential of using the produced zeolite to recover REEs from a secondary source (phosphogypsum leachate). Based on the physicochemical characterization and adsorption data of the ZSM-5, the mechanism was also elucidated. As far as we know, ZSM-5 was never studied as an adsorbent for adsorbing Ce^{3+} , La^{3+} , and Nd^{3+} and extracting REEs from real phosphogypsum leachate samples, which further justifies this work. Thus, we hope this work can serve as a strategy that generates further studies on the development of high-performance adsorbents that can be successfully used in tackling wastewater pollution and extraction of REEs.

2. Materials and methods

2.1. Chemical reagents, preparation, and quantification of REEs synthetic solutions

The analytical grade reagents such as sulfuric acid (H_2SO_4 , 95.0 %), Sodium silicate (Na_2SiO_3 , Na_2O : 53 %; SiO_2 : 47 %), fumed silica [SiO_2 (Aerosil) (0.2–0.3 mm)], aluminum sulfate [$\text{Al}_2(\text{SO}_4)_3$], sodium hydroxide (NaOH , 99.0 %) and tetrapropylammonium hydroxide (TPAOH (20 % v/v)) were purchased from Sigma Aldrich (Germany) and VETEC (Brazil). Cerium(III) nitrate hexahydrate, neodymium(III) nitrate hexahydrate, and lanthanum(III) nitrate hexahydrate (Sigma–Aldrich).

Stock solutions of 1000.0 mg L^{-1} of each REE were prepared using cerium(III) nitrate hexahydrate, neodymium(III) nitrate hexahydrate, and lanthanum(III) nitrate hexahydrate. All the tests were performed by diluting the stock solution in Erlenmeyers. ZSM-5 loaded with REEs was separated by centrifugation (5000 rpm for 5 min). The REEs residual concentrations in the liquid phase were quantified by inductively coupled plasma optical emission spectrometry (ICP-OES) (PerkinElmer, Waltham, MA, United States).

2.2. Synthesis and characterization of ZSM-5 zeolite

The synthesis of the ZSM-5 zeolite was carried out according to the methodology described by Stamires et al. [20], which employs a nucleating gel as an inducer for the formation of the MFI-like structure. This methodology has some advantages, such as a reduced need for TPAOH (an expensive reagent) in the synthesis of the zeolite and a short crystallization time. The molar composition of the synthesis gel was as

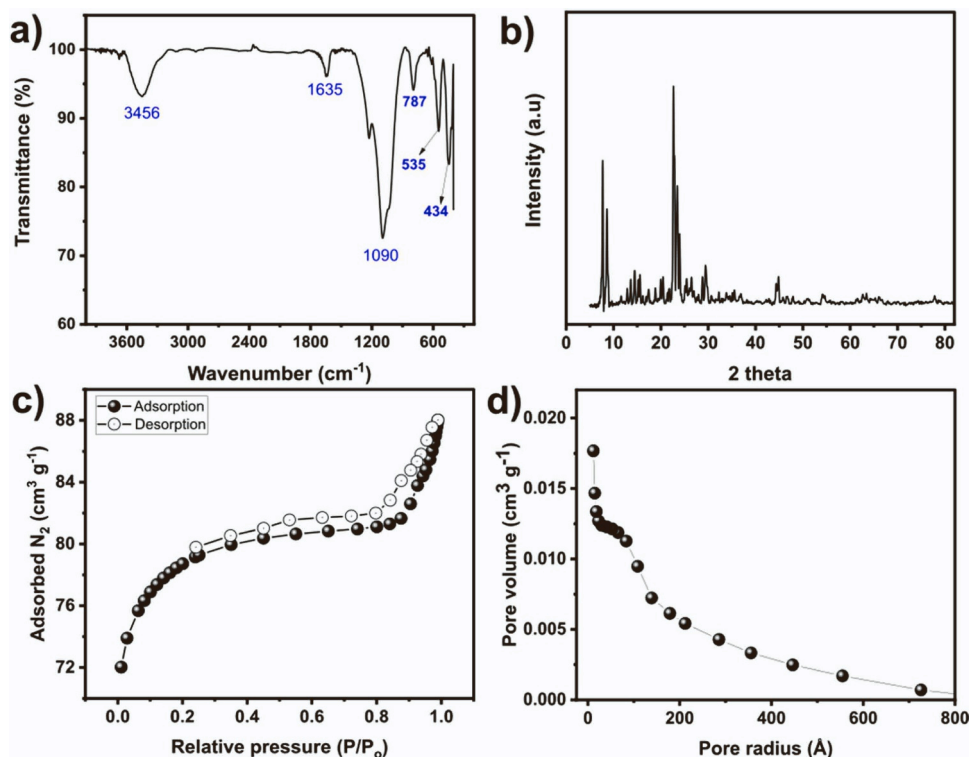


Fig. 1. a) FTIR of the ZSM-5 zeolite, b) XRD of the ZSM-5 zeolite, c) Nitrogen adsorption/desorption isotherms of the ZSM-5 zeolite, and d) pore size distribution curve of the ZSM-5 zeolite.

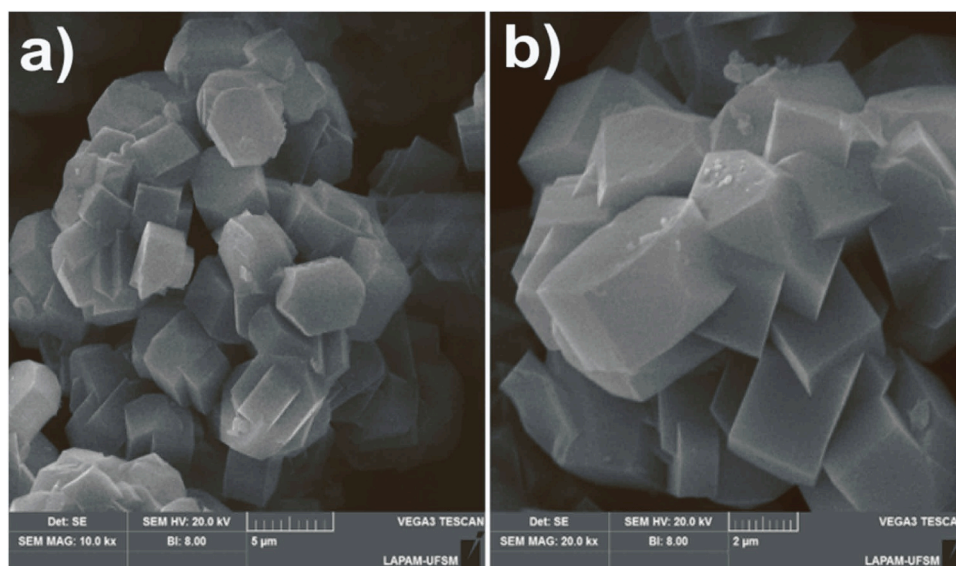


Fig. 2. SEM images of the ZSM-5 zeolite.

follows: SiO_2 : 0.033 Al_2O_3 : 0.6 Na_2O : 0.001 TPA2O: 25 H_2O : 0.2 OH $^-$. The nucleating gel was prepared with the following molar composition: SiO_2 : 0.3 Na_2O : 0.05 TPA2O: 24 H_2O : 0.3 OH $^-$. These compositions were chosen in order to result in a zeolite with a Si/Al ratio equal to 30. Na_2SiO_3 and SiO_2 were used as a source of silicon, and $\text{Al}_2(\text{SO}_4)_3$ was used as a source of aluminum. TPAOH was used to prepare the nucleating gel. Concentrated sulfuric acid was employed to reduce the alkalinity of the medium so that the content of free OH $^-$ ions reached the previously defined level. Initially, the synthesis gel was prepared based on the previously established stoichiometric quantities, and at the end of the process, 1% (by mass) of nucleating gel was added. The

crystallization of the synthesis gel was performed by the static hydrothermal method inside Teflon containers coupled to a stainless steel autoclave at 170 °C for 24 h. Afterward, the formed solid was washed with deionized water and dried for 12 h at 110 °C.

2.3. REEs adsorption experiments

The full experimental description of the batch adsorption followed as reported in [16,21,22], and they are completely detailed in the [supplementary material](#), as well as information about kinetic, equilibrium, and thermodynamic calculations (see [supplementary material](#)). In brief,

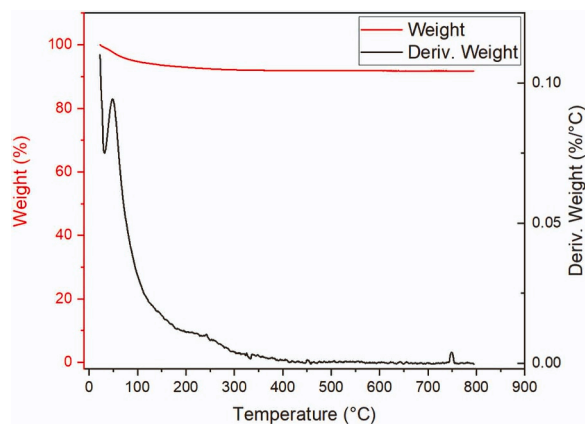


Fig. 3. Thermogravimetric analysis of the ZSM-5 zeolite.

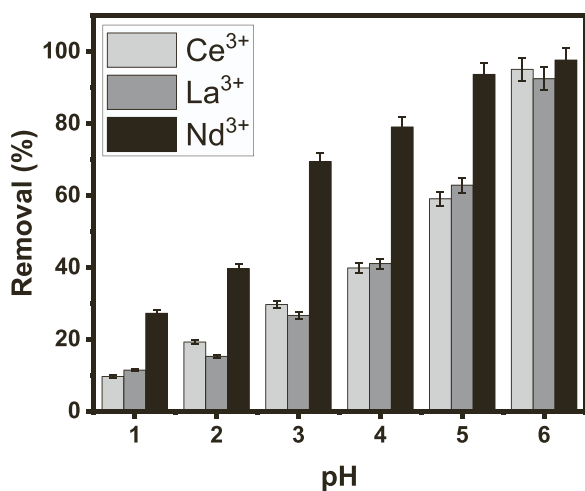


Fig. 4. Effect of the pH on the adsorption of Ce^{3+} , La^{3+} , and Nd^{3+} . Conditions: $C_0 = 50 \text{ mg L}^{-1}$, temperature = 298 K, adsorbent dosage = 1 g L^{-1} and contact time = 2 h.

the adsorption tests were made in discontinuous mode under different conditions of pH metal concentration, contact time, and temperature. All the experiments were carried out in triplicate to ensure reproducibility, reliability, and accuracy of the experimental data. The relative standard deviations of all measurements were below 4%.

2.4. REEs concentration from the phosphogypsum leachate

ZSM-5 was employed to extract the three REEs from real phosphogypsum leachate, which was obtained from a mining abandoned pile located in the southern part of Brazil [16,21,22]. The phosphogypsum was put in contact with citric acid to leach out the REEs into the acid solution to form a liquor [16,21,22]. The leached liquor containing several REEs was characterized in terms of REEs identification and concentration as follows: Ce (150.2 mg L^{-1}), Dy (1.0 mg L^{-1}), Eu (1.2 mg L^{-1}), Gd (2.3 mg L^{-1}), La (70.3 mg L^{-1}), Nd (55.4 mg L^{-1}), Pr (10.4 mg L^{-1}), Sm (7.6 mg L^{-1}), and Y (1.0 mg L^{-1}). It was worthwhile to stress that the liquor is strongly acidic (pH 1), and Ca in elevated concentration is found. Thus, 100 mL of the liquor was injected with 200 mg of ZSM-5 (2 g L^{-1}) for 8 h at 298 K and 250 rpm.

3. Results and discussion

3.1. ZSM-5 physicochemical features

FTIR was employed to identify the presence of functional groups on the surface of ZSM-5 adsorbent—it enables a better understanding of the surface features, which have a huge impact on the adsorption properties since the functional groups serve as adsorption site for binding ions and molecules. The FT-IR analysis of the ZSM-5 zeolite is shown in Fig. 1a.

The bands at 434 and 535 cm^{-1} can be assigned to bending vibrations of internal Al/Si-O bonds of AlO_4 and SiO_2 [23]. The band at approximately 787 cm^{-1} can be assigned to symmetrical stretching of the external Si-O-Al/Si bonds, and the band at 1090 cm^{-1} can be assigned to internal asymmetric stretching of Si-O-Si/Al bonds. External asymmetric stretching of four-chain structures formed by five-membered rings can be assigned to adsorption bands in the region of 1200 cm^{-1} . The band that occurs at 1635 cm^{-1} could be related to the vibrations of the O-H group [24]. The band seen at approximately 3400 cm^{-1} is assigned to water molecules adsorbed on the zeolite surface. The ZSM-5 has shown the presence of many functionalities on its surface, which could positively impact the removal of ions such REEs.

The XRD analysis of the ZSM-5 zeolite (Fig. 1b) corresponds to an MFI structure with characteristic diffraction peaks of calcined zeolites [25]. The structure indicates the orthorhombic end member of the pentasil family of zeolites, which suggests the formation of the ZSM-5 zeolite [26]. The diffractogram also shows that the ZSM-5 zeolite is totally crystalline due to the absence of a broad humped zone at low angles.

The porosity features (specific surface area and the amount of micropores) are highly important characteristics of an adsorbent, which usually play a huge influence on the materials' ability to adsorb ions/molecules [22,27]. Nitrogen adsorption-desorption isotherms (N_2 physisorption) of the ZSM-5 zeolite (Fig. 1c) illustrate a hybrid type I/IV behavior. Type I contribution is due to the high N_2 uptake at low partial pressure, which is due to a big amount of micropores; type IV is due to the presence of a hysteresis loop at higher partial pressures, behavior that is typical of materials with mesoporous structures. The S_{BET} is approximately $264 \text{ m}^2 \text{ g}^{-1}$, of which $225 \text{ m}^2 \text{ g}^{-1}$ correspond to micropores and $39 \text{ m}^2 \text{ g}^{-1}$ to mesopores. The pore size distribution derived from the BJH model (Fig. 1d) shows that the majority of the pore volume is within pores with a radius of 12–200 Å.

SEM analysis provides valuable information on the morphology of the adsorbent materials that can be used to understand their adsorptive performances. SEM imaging at different magnifications is shown in Fig. 2 and it reveals that the surface of the ZSM-5 zeolite is highly irregular, composed of crystals with varied shapes and sizes. The material is dominated by hexagonal prism-shaped crystals, which are 3–5 micrometers long, which is in accordance with the literature [28]. The spaces and cavities scattered randomly across the surface can increase the surface area available for uptaking molecules/ions, thus boosting the adsorption performances.

The thermal stability of the ZSM-5 material was evaluated by TGA analysis (see Fig. 3). The TGA curve shows a very temperature-stable structure of zeolite material with only 8% mass loss even reaching high temperatures (800°C). The weight loss can be attributed to bound water that is liberated from the zeolite during the heat treatment that accrued mainly at the temperature up to 200°C . This result is in accordance with the results reported by Schnee et al. [29] who studied a similar zeolite material.

3.2. pH effect on the REEs adsorption

The pH of the solution of REEs plays an essential role during the adsorption process because it affects the ionization of functional groups on the surface of the adsorbent [22,30]. Experiments were carried out using REEs solutions with pH from 1 to 6. The results for the adsorption

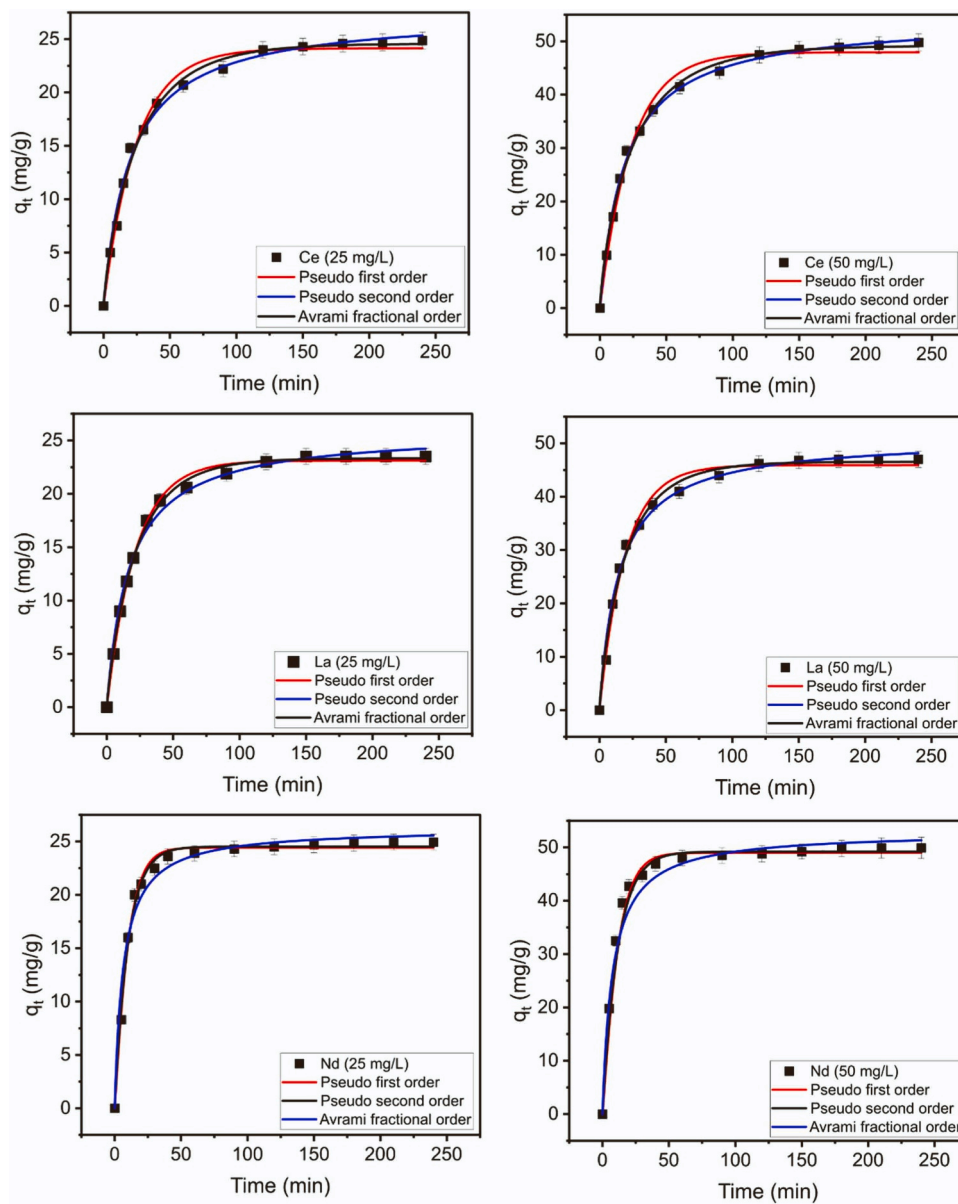


Fig. 5. Kinetics of adsorption of Ce, La, and Nd onto ZSM-5 zeolite at different initial concentrations. Conditions: pH = 6, 298 K, adsorbent dosage = 1 g L⁻¹.

Table 1
Kinetic parameters of Ce³⁺, La³⁺, and Nd³⁺ adsorption onto ZSM-5.

C ₀ (mg L ⁻¹)	25	50
Cerium (Ce)		
Pseudo-first-order		
q _e (mg g ⁻¹)	24.14	47.94
k ₁ (min ⁻¹)	0.041	0.042
R _{adj} ²	0.991	0.989
SD (mg g ⁻¹)	0.805	1.676
Pseudo-second-order		
q _e (mg g ⁻¹)	27.48	54.29
k ₂ (g mg ⁻¹ min ⁻¹)	0.002	9.679 E-4
R _{adj} ²	0.993	0.997
SD (mg g ⁻¹)	0.665	1.163
Avrami fractional order		
q _e (mg g ⁻¹)	24.58	49.21
k _a (g mg ⁻¹ min ⁻¹)	0.038	0.038
n	0.852	0.803
h ₀	0.58	0.87
R _{adj} ²	0.991	0.995
SD (mg g ⁻¹)	0.636	0.96
Lanthanum (La)		
Pseudo-first-order		
q _e (mg g ⁻¹)	23.11	45.91
k ₁ (min ⁻¹)	0.046	0.052
R _{adj} ²	0.996	0.989
SD (mg g ⁻¹)	0.685	1.525
Pseudo-second-order		
q _e (mg g ⁻¹)	25.92	51.12
k ₂ (g mg ⁻¹ min ⁻¹)	0.002	0.001
R _{adj} ²	0.993	0.993
SD (mg g ⁻¹)	0.604	1.301
Avrami fractional order		
q _e (mg g ⁻¹)	23.33	46.55
k _a (g mg ⁻¹ min ⁻¹)	0.045	0.049
n	0.894	0.853
h ₀	0.75	1.3
R _{adj} ²	0.997	0.992
SD (mg g ⁻¹)	0.392	1.019
Neodymium (Nd)		
Pseudo-first-order		
q _e (mg g ⁻¹)	24.52	48.83
k ₁ (min ⁻¹)	0.099	0.106
R _{adj} ²	0.993	0.996
SD (mg g ⁻¹)	0.626	0.938
Pseudo-second-order		
q _e (mg g ⁻¹)	26.25	52.06
k ₂ (g mg ⁻¹ min ⁻¹)	0.006	0.003
R _{adj} ²	0.974	0.986
SD (mg g ⁻¹)	1.196	1.724
Avrami fractional order		
q _e (mg g ⁻¹)	24.42	48.98
k _a (g mg ⁻¹ min ⁻¹)	0.099	0.087
n	1.092	1.112
h ₀	3.2	6.6
R _{adj} ²	0.993	0.996
SD (mg g ⁻¹)	0.525	0.842

of Ce³⁺, La³⁺, and Nd³⁺ are presented in Fig. 4. The adsorption capacity (q) increases with the increase of the pH, and the highest adsorption capacities were obtained at pH 6 for all elements.

At a low pH, the removal of these REEs is low due to the active sites being occupied by H⁺ that compete with the REEs. Also, at low pH, the strong electrostatic repulsion between the positively charged zeolite and the REEs occurs, hindering the adsorption process. By increasing the pH, the removal of the REEs from the solution increases due to the decrease of H⁺ in the aqueous solution, which reduces the competition with the REEs and enhances adsorption. At pH 6, almost complete removal of the three REEs was achieved from solutions with an initial concentration of 50 mg/L when using an adsorbent dosage of 1 g L⁻¹.

3.3. Kinetics of REEs adsorption

The kinetics of adsorption is a very important step of any adsorption

process for elucidating the mechanism(s) involved in the process, such as diffusion control and mass transport processes. It also gives crucial information to understand the efficiency and practicability of an adsorbent and to better design a highly effective adsorption process.

Two initial concentrations were employed for the kinetics of Ce³⁺, La³⁺, and Nd³⁺ onto ZSM5 adsorbent (see Fig. 5). Firstly, a typical kinetic profile is observed for the three REEs, where the adsorption capacity increased over time. The adsorption capacities behaviors of the REEs did not differ much over time, with values around 25 mg g⁻¹ and 50 mg g⁻¹ for 25 and 50 mg L⁻¹, respectively.

The nonlinear pseudo-first order, pseudo-second order, and Avrami fractional order kinetic models were used for the evaluation of the experimental measurements (Fig. 5). The models' ability to fit the experimental points was judged based on the R_{adj}² and SD parameters [22,31–33]. A higher R_{adj}² and lower SD values mean a lower discrepancy between the experimental q value and the one predicted by the model and, therefore, a better fit of the model to the experimental data.

The curves of kinetic data are displayed in Fig. 5, and their parameters are shown in Table 1. Based on Fig. 6 and Table 2 results, the Avrami-fractional order displayed the highest R_{adj}² and lowest SD values, and thus, it was the best-suited model to describe the kinetics of adsorption for the three REEs (Ce³⁺, La³⁺, and Nd³⁺) onto the ZSM-5 adsorbent. The Avrami model is world widely employed to understand kinetic processes [33–35]. The suitability of the Avrami model indicates a complex process with different kinetic pathways in which the mechanism (s) change while the adsorption is taking place [33–35].

This model may follow multiple different kinetic orders (instead of one), in which changes occur during the contact between REEs (Ce³⁺, La³⁺, and Nd³⁺) and ZSM5. Moreover, the Avrami equation exponent (n_{AV}) indicates the multiple adsorption kinetic orders that commonly have a fractional value [33–35].

Taking into account the Avrami-fractional order complexity in understanding its own parameters, such as the constant kinetic rate (k). To better understand the kinetics' behavior of Ce³⁺, La³⁺, and Nd³⁺ onto ZSM-5, the sorption rate (h₀) was accessed [16], which is shown by the Equation (1): h₀ = k_n · q_eⁿ (see Equation's details in the supplementary material). For the calculation of h₀, the Equation's parameters were taken from the best-fitted model [16]. The h₀ values for higher for Nd³⁺ followed by La³⁺ and Ce³⁺ (See Table 1), which suggests that the fastest kinetics was for Nd³⁺ followed by La³⁺ and Ce³⁺.

3.4. Equilibrium and thermodynamics of REEs adsorption

To properly study the equilibrium process of an adsorption system, it is crucial to deeply understand the relationship between an adsorbate (e. g., REEs) at different initial concentrations and its degree of accumulation onto the adsorbent surface at a constant temperature. Moreover, it gives valuable insights into the effectiveness of an adsorbent because it gives its maximum adsorption capacity; thus, it enables to design of an efficient adsorption process.

The results obtained from the equilibrium isotherms of adsorption measurements at temperatures ranging from 298 K to 328 K are shown in Fig. 6. The experimental points were fitted using the nonlinear Langmuir, Freundlich, and Liu models, respectively. The suitability of the models was also judged based on the R_{adj}² and SD parameters. According to the results shown in Table 2, the Liu model demonstrated the best fit to the experimental data. This isotherm is a combination of the Langmuir and Freundlich isotherm and suggests a complex adsorption mechanism with different pathways. The Langmuir model exhibited SD and R_{adj}² values closer to those of the Liu model, compared to Freundlich, suggesting that the adsorption process is more homogeneous than heterogeneous.

It was observed that for all curves, enhancing the temperature provoked a drop in the maximum adsorption removal (See Fig. 6 and Table 2), highlighting the negative effect of the temperature on their uptake. Further discussion is provided in the next section,

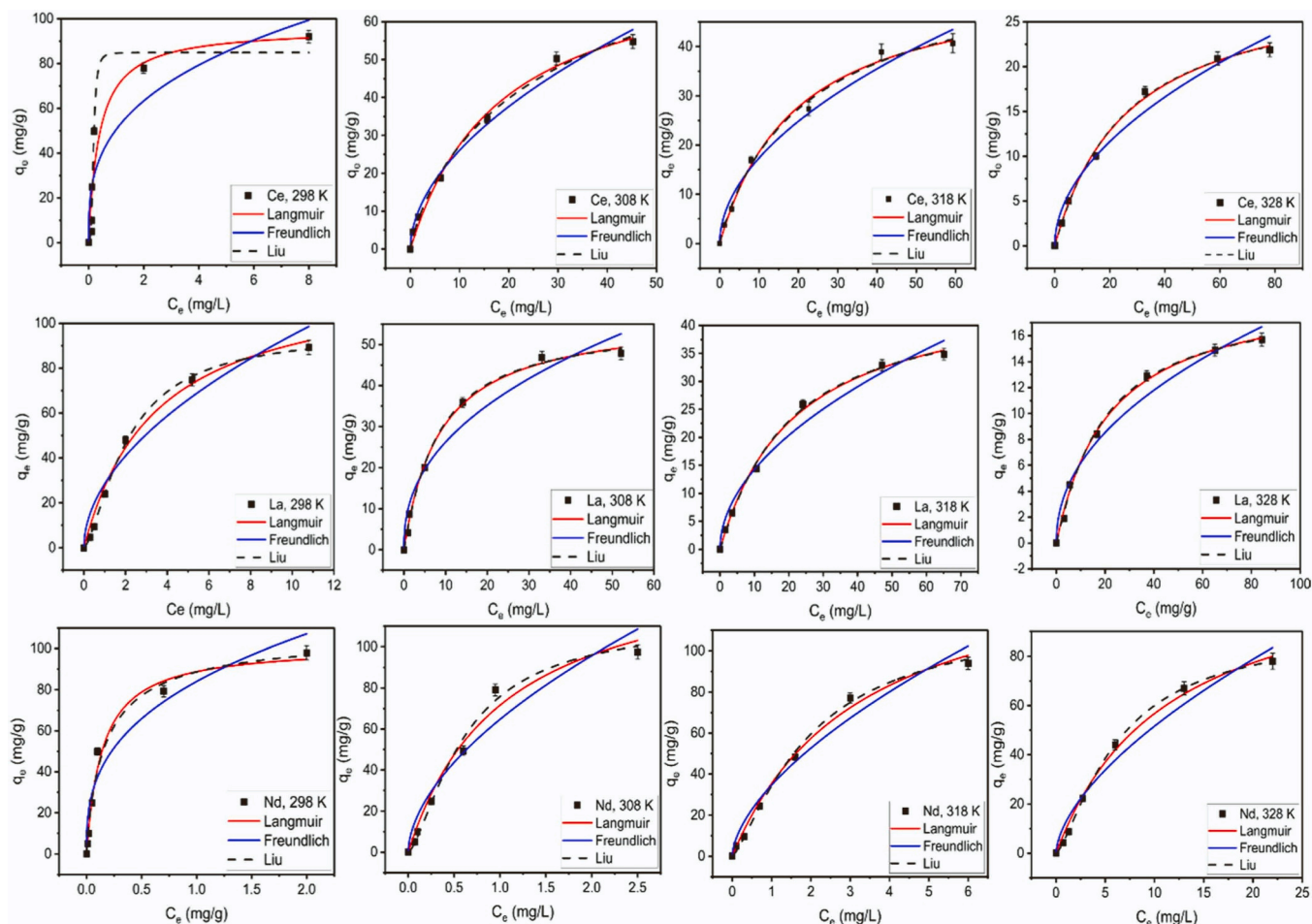


Fig. 6. Isotherms of adsorption of Ce, La, and Nd onto ZSM-5 zeolite.

"Thermodynamic studies." The equilibrium isotherms have shown that ZSM-5 demonstrated remarkable efficiencies in the removal of the three REEs. A way to better access the ZSM-5 adsorptive performance is to compare it with the adsorptive metrics of other adsorbents reported in the literature. In this regard, Table 3 shows a comparison between ZSM-5 and other adsorbents [36–44]. Assuming all adsorption data were obtained through best-optimized conditions, ZSM-5 displayed a very competitive level of removals for the three REEs (See Table 3).

A much better performance was achieved by an adsorbent based on lanthanum ion imprinted polymer [39], which exhibited a much higher q_{max} value for REEs. However, it is worthwhile to state that this adsorbent faces issues regarding a much more complex synthesis process and high use of chemicals and energy that reflect in higher costs that hinder its real application; instead, zeolite is an abundant, natural, low-cost, and effective adsorbent with enormous effectiveness real application in removing/extracting REEs from a synthetic and real application.

3.5. Thermodynamic studies of Ce^{3+} , La^{3+} , and Nd^{3+} on ZSM-5

For the right evaluation of the influence of temperature on an adsorption process, it is desired and important to calculate the thermodynamic process data, which brings important insights in relation to

the adsorption's nature regarding spontaneity, feasibility, randomness, exothermicity or endothermicity [21,22,31–33]. Table 4 shows the thermodynamic adsorption parameters of ZSM-5 adsorbent material for the three REEs (Ce^{3+} , La^{3+} , and Nd^{3+}).

The data in Table 4 suggest that the uptake of Ce^{3+} , La^{3+} , and Nd^{3+} onto ZSM-5 was spontaneous for all four temperatures (298, 308, 318, and 328 K) due to the negative ΔG^0 values [21,22,31–33]. Further, when studying the adsorption process, the ΔH^0 values are higher than 0, and thus, the adsorption process was endothermic for all three REEs. Moreover, the ΔH^0 values indicate magnitudes of the adsorption for three REEs onto ZSM-5 compatible with ion exchange [16,21].

Finally, for all three REEs, the values of the changes in the entropy (ΔS^0) were negative, suggesting a diminution of the randomness and a more organized state of the adsorption system after the Nd^{3+} , Ce^{3+} and La^{3+} are adsorbed by ZSM-5, adsorbent material [16,21,46–49].

3.6. REEs concentration from the PG leachate

The suitability of the ZSM-5 zeolite for its use as an adsorbent for the recovery of REEs in real conditions was determined using phosphogypsum leachate. Fig. 7 shows the influence of the adsorbent dose on the adsorption capacity (q) and the corresponding percentage of removal.

Table 2
Isotherm parameters for adsorption of Ce³⁺, La³⁺, and Nd³⁺ onto ZSM-5.

	298 K	308 K	318 K	328 K
Cerium (Ce)				
Langmuir				
Q _{max} (mg g ⁻¹)	95.87	78.42	54.83	29.99
K _L (L mg ⁻¹)	2.574	0.054	0.051	0.037
R _{adj} ²	0.908	0.993	0.994	0.996
SD (mg g ⁻¹)	11.12	1.907	1.539	0.929
Freundlich				
K _F ((mg g ⁻¹) (mg L ⁻¹) ^{-1/n})	50.48	7.701	5.293	2.497
n _F	3.071	1.889	1.939	1.947
R _{adj} ²	0.821	0.987	0.979	0.975
SD (mg g ⁻¹)	15.63	2.534	2.406	1.434
Liu				
Q _{max} (mg g ⁻¹)	99.42	84.89	59.42	28.82
K _L (L mg ⁻¹)	2.652	1.031	0.062	0.041
n _L	3.328	0.819	0.921	1.051
R _{adj} ²	0.966	0.993	0.992	0.994
SD (mg g ⁻¹)	6.739	1.841	1.347	0.678
Lanthanum (La)				
Langmuir				
Q _{max} (mg g ⁻¹)	121.8	57.44	47.51	19.87
K _L (L mg ⁻¹)	0.288	0.114	0.046	0.046
R _{adj} ²	0.988	0.996	0.997	0.996
SD (mg g ⁻¹)	3.939	1.364	0.983	0.889
Freundlich				
K _F ((mg g ⁻¹) (mg L ⁻¹) ^{-1/n})	28.49	9.942	4.381	2.108
n _F	1.917	2.372	1.949	2.143
R _{adj} ²	0.939	0.951	0.974	0.968
SD (mg g ⁻¹)	8.758	4.479	2.311	1.137
Liu				
Q _{max} (mg g ⁻¹)	96.43	55.76	45.25	18.96
K _L (L mg ⁻¹)	0.475	0.123	0.051	0.032
n _L	1.476	1.059	1.064	1.073
R _{adj} ²	0.999	0.995	0.996	0.994
SD (mg g ⁻¹)	1.055	1.261	0.841	0.414
Neodymium (Nd)				
Langmuir				
Q _{max} (mg g ⁻¹)	101.6	145.8	151.2	121.4
K _L (L mg ⁻¹)	6.899	0.964	0.306	0.088
R _{adj} ²	0.984	0.981	0.994	0.993
SD (mg g ⁻¹)	4.937	5.568	3.134	2.684
Freundlich				
K _F ((mg g ⁻¹) (mg L ⁻¹) ^{-1/n})	84.02	64.68	34.62	12.67
n _F	2.847	1.768	1.653	1.639
R _{adj} ²	0.943	0.941	0.972	0.963
SD (mg g ⁻¹)	9.322	9.977	6.601	6.059
Liu				
Q _{max} (mg g ⁻¹)	118.1	113.1	108.6	92.07
K _L (L mg ⁻¹)	5.638	1.623	0.503	0.157
n _L	0.879	1.466	1.311	1.375
R _{adj} ²	0.983	0.991	0.997	0.999
SD (mg g ⁻¹)	4.132	4.052	2.219	0.455

The highest adsorption capacity for Ce (32 mg g⁻¹), corresponding to a recovery of around 84 %, was obtained using a sample dose of 5 g L⁻¹. For La, the maximum adsorption capacity (12 mg g⁻¹) with a recovery of around 75 % was also obtained using a sample dose of 5 g L⁻¹. When using the same adsorbent dose, the q for Nd was approximately 20 mg g⁻¹, which corresponds to a percentage of removal of around 97 %. Adsorbent doses higher than 5 g L⁻¹ result in removals of nearly 100 %, but the adsorption capacity (q) is reduced drastically, meaning that adsorbent doses higher than 5 g L⁻¹ are probably not justified economically speaking.

4. Conclusions

Herein, we demonstrated that ZSM-5 zeolite could be successfully employed as an adsorbent to remove La³⁺, Ce³⁺, and Nd³⁺. The suitability of the ZSM-5 zeolite for its use as an adsorbent for the recovery of REEs in real conditions was determined using phosphogypsum leachate. The maximum adsorption capacity for Ce³⁺, La³⁺, and Nd³⁺ were 99.42 mg g⁻¹, 96.43 mg g⁻¹, 118.10 mg g⁻¹, respectively. The

Table 3
Comparison of the Q_{max} for REEs using different adsorbents.

Adsorbents	Q _{max} (mg g ⁻¹)	REEs	pH	Ref.
Zeolite-based from kaolinite	53	Ce ³⁺	6.0	[36]
Adsorbent based on Bacillus licheniformis	39	Ce ³⁺	6.0	[37]
Magnetic nanocomposite	91	Ce ³⁺	6.0	[38]
La-ion imprinted polymer	563	La ³⁺	5.0	[39]
Nano-magnetite functionalized with H ₃ PO ₃ group	20	La ³⁺	6.0	[40]
Durian rind	41	La ³⁺	4.0	[41]
CA/P(P-T-A)/NZFO	71	Nd ³⁺	5.5	[42]
Lanthanide-ion imprinted polymer adsorbent	126	Nd ³⁺	6.0	[43]
CA@Fe3O4 NPs	41	Nd ³⁺	7.0	[44]
Diatomite	23	La ³⁺	2.0	[45]
Diatomite	56	Ce ³⁺	2.0	[45]
Diatomite	101	Nd ³⁺	2.0	[45]
ZSM-5	99.4	La ³⁺	6.0	This work
	96.4	Ce ³⁺		
	118.1	Nd ³⁺		

Table 4
Thermodynamic parameters of Nd³⁺, Ce³⁺, and La³⁺ on ZSM-5.

T (K)	ΔG ⁰ (kJ mol ⁻¹)	ΔH ⁰ (kJ mol ⁻¹)	ΔS ⁰ (J mol ⁻¹ K ⁻¹)
Ce³⁺			
298	-31.68		
308	-30.42	98.2	-223.1
318	-27.79		
328	-25.10		
La³⁺			
298	-27.49		
308	-24.96	73.3	-155.5
318	-23.44		
328	-22.91		
Nd³⁺			
298	-33.72	96.8	
308	-31.66		-211.6
318	-29.59		
328	-27.34		

thermodynamic study indicated a favorable, spontaneous, and endothermic adsorption process. When employed to recover several REEs from leachate of phosphogypsum wastes, the ZSM-5 showed high performance in recovering such REEs. The findings reported in this work support the idea that ZSM-5 can be successfully used as an adsorbent to recover REEs from synthetic and real samples.

CRedit authorship contribution statement

Mohammad Rizwan Khan: Writing – review & editing. **Naushad Ahmad:** Writing – review & editing. **Irineu A.S. de Brum:** Writing – review & editing. **Guilherme Luiz Dotto:** Writing – original draft, Data curation, Conceptualization. **Diana Pinto:** Writing – review & editing, Formal analysis. **Luis Felipe Oliveira Silva:** Writing – review & editing. **Alejandro Grimm:** Writing – review & editing, Data curation. **Jyri-Pekka Mikkola:** Writing – review & editing. **Glaydson Simões dos Reis:** Writing – review & editing, Writing – original draft, Visualization, Validation, Data curation.

Declaration of Competing Interest

The authors declare the following financial interests/personal relationships which may be considered as potential competing interests: Glaydson Simoes dos Reis reports financial support was provided by Swedish University of Agricultural Sciences. If there are other authors, they declare that they have no known competing financial interests or personal relationships that could have appeared to influence the work

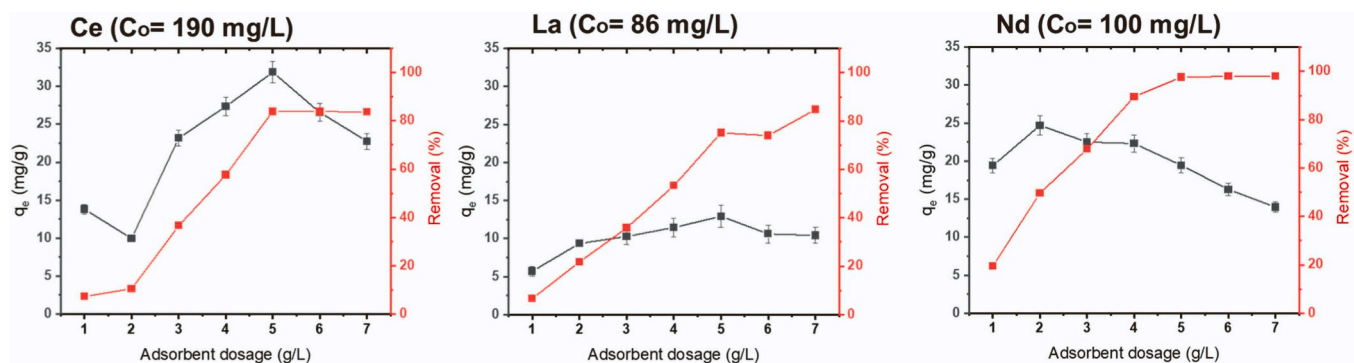


Fig. 7. Adsorption of cerium, lanthanum, and neodymium from phosphogypsum leachate.

reported in this paper.

Data availability

Data will be made available on request.

Acknowledgments

This work was funded by the Brazilian National Council for Scientific and Technological Development/CNPq (Grant 405982/2022-4 and Grant 303992/2021-2) and Coordination for the Improvement of Higher Education Personnel/CAPES (Financial code 001). Financial support from the Swedish Research Council FORMAS (grant No. 2021-00877) is acknowledged. This work is also a part of activities of the Technical Chemistry Department of Chemistry, Chemical-Biological Centre, Umeå University, Sweden, and the Laboratory of Industrial Chemistry and Reaction Engineering, Johan Gadolin Process Chemistry Centre at Åbo Akademi University, Finland. The Swedish Bio4Energy program is gratefully acknowledged. The authors would like to thank the Researchers Supporting Project number (RSPD2024R668), King Saud University, Riyadh, Saudi Arabia.

Appendix A. Supporting information

Supplementary data associated with this article can be found in the online version at [doi:10.1016/j.colsurfa.2024.134549](https://doi.org/10.1016/j.colsurfa.2024.134549).

References

- [1] V. Fernandez, Rare-earth elements market: a historical and financial perspective, *Resour. Policy* 53 (2017) 26–45, <https://doi.org/10.1016/j.resourpol.2017.05.010>.
- [2] M.A. de Boer, K. Lammertsma, Scarcity of rare earth elements, *ChemSusChem* 6 (2013) 2045–2055.
- [3] T.Z. Humsa, R.K. Srivastava, Impact of rare earth mining and processing on soil and water environment at Chavara, Kollam, Kerala: a case study, *Procedia Earth Planet. Sci.* 11 (2015) 566–581, <https://doi.org/10.1016/j.proeps.2015.06.059>.
- [4] J. Li, K. Peng, P. Wang, N. Zhang, K. Feng, D. Guan, J. Meng, W. Wei, Q. Yang, Critical Rare-Earth Elements Mismatch Global WindPower Ambitions, *One Earth* 3 (2020) 116–125.
- [5] V. Balam, Rare earth elements: a review of applications, occurrence, exploration, analysis, recycling, and environmental impact, *Geosci. Front.* 10 (2019) 1285–1303.
- [6] J. Kulczycka, Z. Kowalski, M. Smol, H. Wirth, Evaluation of the recovery of rare earth elements (REE) from phosphogypsum waste case study of the WIZOW chemical plant (Poland), *J. Clean. Prod.* 113 (2016) 345–354.
- [7] V.N. Rychkov, E.V. Kirillov, S.V. Kirillov, V.S. Semenishchev, G.M. Bunkov, M. S. Botalov, D.V. Smyshlyayev, A.S. Malyshev, Recovery of rare earth elements from phosphogypsum, *J. Clean. Prod.* 196 (2018) 674–681.
- [8] R.K. Jyothi, T. Thenepalli, J.W. Ahn, P.K. Parhi, K.W. Chung, J.Y. Lee, Review of rare earth elements recovery from secondary resources for clean energy technologies: grand opportunities to create wealth from waste, *J. Clean. Prod.* 267 (2020) 122048, <https://doi.org/10.1016/j.jclepro.2020.122048>.
- [9] Abhilash, P. Meshram, S. Sarkar, T. Venugopalan, Exploring blast furnace slag as a secondary resource for extraction of rare earth elements, *Miner. Metall. Process.* 34 (2017) 178–182, <https://doi.org/10.19150/mmp.7857>.
- [10] S. Panda, R.B. Costa, S.S. Shah, S. Mishra, D. Bevilacqua, A. Akcil, Biotechnological trends and market impact on the recovery of rare earth elements from bauxite residue (red mud)—a review, *Resour., Conserv. Recycl.* 171 (2021) 105645, <https://doi.org/10.1016/j.resconrec.2021.105645>.
- [11] S. Peelman, Z.H. Sun, J. Sietsma, Y. Yang, Leaching of rare earth elements: review of past and present technologies, *Rare Earths Ind.* (2016) 319–334, <https://doi.org/10.1016/B978-0-12-802328-0.00021-8>.
- [12] Z. Hammache, S. Bensaadi, Y. Berbar, N. Audebrand, A. Szymczyk, M. Amara, Recovery of rare earth elements from electronic waste by diffusion dialysis, *Sep. Purif. Technol.* 254 (2021) 117641, <https://doi.org/10.1016/j.seppur.2020.117641>.
- [13] S.F. Lütke, M.L.S. Oliveira, S.R. Waechter, L.F.O. Silva, T.R.S. Cadaval Jr., F. A. Duarte, G.L. Dotto, Leaching of rare earth elements from phosphogypsum, *Chemosphere* 301 (2022) 134661.
- [14] R.F. Pinheiro, A. Grimm, M.L.S. Oliveira, J. Vieillard, L.F.O. Silva, I.A.S. De Brum, E.C. Lima, M. Naushad, L. Selloui, G.L. Dotto, G.S. dos Reis, Adsorptive behavior of the rare earth elements Ce and La on a soybean pod derived activated carbon: application in synthetic solutions, real leachate and mechanistic insights by statistical physics modeling, *Chem. Eng. J.* 471 (2023) 144484.
- [15] G.L. Dotto, J. Vieillard, D. Pinto, S.F. Lütke, L.F.O. Silva, G.S. dos Reis, E.C. Lima, D.S.P. Franco, Selective adsorption of gadolinium from real leachate using a natural bentonite clay, *J. Environ. Chem. Eng.* 11 (2023) 109748.
- [16] G.S. dos Reis, V. Srivastava, M.F.A. Taleb, et al., Adsorption of rare earth elements on a magnetic geopolymer derived from rice husk: studies in batch, column, and application in real phosphogypsum leachate sample, *Environ. Sci. Pollut. Res.* (2024), <https://doi.org/10.1007/s11356-024-31925-x>.
- [17] Walawalkar, K.Nichol Connie, Process investigation of the acid leaching of rare earth elements from phosphogypsum using HCl, HNO₃, and H₂SO₄, *Hydrometallurgy* 166 (2016) 195–204, <https://doi.org/10.1016/j.hydromet.2016.06.008>.
- [18] A. Khaleque, M.M. Alam, M. Hoque, S. Mondal, J.B. Haider, B. Xu, M.A.H. Johir, A. K. Karmakar, J.L. Zhou, M.B. Ahmed, M.A. Moni, Zeolite synthesis from low-cost materials and environmental applications: a review, *Environ. Adv.* 2 (2020) 100019.
- [19] E. Perez-Botella, S. Valencia, F. Rey, Zeolites in adsorption processes: state of the art and future prospects, *Chem. Rev.* 122 (2022) 17647–17695.
- [20] D. Stamiros, Y. L. lam, J. Gorne, R. Wasserman, J.C.M. Ferreira, J. da Silva, Nucleating gel, process for its preparation, and its use in the synthesis of MFI-type zeolite. Patent Cooperation Treaty (PCT), no. WO/2006/087337, 2006. Available from: < <https://patentscope.wipo.int/search/en/detail.jsf?docId=WO2006087337>>
- [21] G.S. dos Reis, C.E. Schnorr, G.L. Dotto, J. Vieillard, M.S. Netto, L.F.O. Silva, I.A.S. De Brum, M. Thyrel, E.C. Lima, U. Lassi, Wood waste-based functionalized natural hydrochar for the effective removal of Ce(III) ions from aqueous solution, *Environ. Sci. Pollut. Res.* 30 (2023) 64067–64077.
- [22] G.S. dos Reis, D. Pinto, E.C. Lima, S. Knani, A. Grimm, L.F.O. Silva, T.R. S. Cadaval Jr, G.L. Dotto, Lanthanum uptake from water using chitosan with different configurations, *React. Funct. Polym.* 180 (2022) 105395.
- [23] H. Jedli, M.M. Almoneeff, M. Mbarek, A. Jbara, K. Slimi, Adsorption of CO₂ onto zeolite ZSM-5: kinetic, equilibrium and thermodynamic studies, *Fuel* 321 (2022) 124097.
- [24] W. Panpa, S. Jinawath, Synthesis of ZSM-5 zeolite and silicalite from rice husk ash, *Appl. Catal. B* 90 (2009) 389–394.
- [25] S. Bosnar, V. Rac, D. Stosic, A. Travert, G. Postole, A. Auroux, S. Skapin, L. Damjanovic, J. Bronic, X. Du, S. Markovic, V. Pavlovi, V. Rakic, Overcoming phase separation in dual templating: a homogeneous hierarchical ZSM-5 zeolite with flower-like morphology, synthesis and in-depth acidity study, *Microporous Mesoporous Mater.* 329 (2022) 111534.
- [26] L. Chu, G. Liu, Q. Xiao, Direct construction of hierarchical ZSM-5 microspheres aided by 3-glycidoxypropyltrimethoxysilane, *Mater. Res. Bull.* 60 (2014) 746–751.
- [27] P.S. Kumar, L. Korving, K.J. Keesman, Mark C.M. van Loosdrecht, G.-J. Witkamp, Effect of pore size distribution and particle size of porous metal oxides on phosphate adsorption capacity and kinetics, *Chem. Eng. J.* 358 (2019) 160–169.

- [28] Y. Wang, T. Du, X. Fang, H. Jia, Z. Qiu, Y. Song, Synthesis of CO₂-adsorbing ZSM-5 zeolite from rice husk ash via the colloidal pretreatment method, *Mater. Chem. Phys.* 232 (2019) 284–293.
- [29] J. Schnee, M. Quezada, O. Norosoa, F. Azzolina-Jury, ZSM-5 surface modification by plasma for catalytic activity improvement in the gas phase methanol-to-dimethylether reaction, *Catal. Today* 337 (2019) 195–200.
- [30] X. Feng, O. Onel, M. Council-Troche, A. Noble, R.H. Yoon, J.R. Morris, A study of rare earth ion-adsorption clays: the speciation of rare earth elements on kaolinite at basic pH, *Appl. Clay Sci.* 201 (2021) 105920.
- [31] G.S. dos Reis, J. Thivet, E. Laisn'e, V. Srivastava, A. Grimm, E.C. Lima, D. Bergna, T. Hu, M. Naushad, U. Lassi, Synthesis of novel mesoporous selenium-doped biochar with high-performance sodium diclofenac and reactive orange 16 dye removals, *Chem. Eng. Sci.* (2023) 119129, <https://doi.org/10.1016/j.ces.2023.119129>.
- [32] G.S. dos Reis, D. Bergna, A. Grimm, E.C. Lima, H. Hu, M. Naushad, U. Lassi, Preparation of highly porous nitrogen-doped biochar derived from birch tree wastes with superior dye removal performance, *Colloids Surf. A* 669 (2023) 131493, <https://doi.org/10.1016/j.colsurfa.2023.131493>.
- [33] A. Grimm, G.S. dos Reis, V.M. Dinh, S.H. Larsson, J.-P. Mikkola, E.C. Lima, S. Xiong, Hardwood spent mushroom substrate-based activated biochar as a sustainable bioresource for removal of emerging pollutants from wastewater, *Biomass-Bioenerg.* 14 (2022) 2293–2309, <https://doi.org/10.1007/s13399-022-02618-7>.
- [34] R.C. Ferreira, O.M.C. Junior, K.Q. Carvalho, P.A. Arroyo, M.A.S.D. Barros, Effect of solution pH on the removal of paracetamol by activated carbon of dende coconut mesocarp, *Chem. Biochem Eng. Q* 29 (2015) 47–53.
- [35] A.R. Cestari, E.F.S. Vieira, G.S. Vieira, L.E. Almeida, The removal of anionic dyes from aqueous solutions in the presence of anionic surfactant using aminopropyl silica-a kinetic study, *J. Hazard Mater.* 138 (2006) 133–141.
- [36] B. Ji, W. Zhang, Adsorption of cerium (III) by zeolites synthesized from kaolinite after rare earth elements (REEs) recovery, *Chemosphere* 303 (2022) 134941.
- [37] Y. Cheng, T. Zhang, L. Zhang, Z. Ke, L. Kovarik, H. Dong, Resource recovery: Adsorption and biomineralization of cerium by *Bacillus licheniformis*, *J. Hazard. Mat.* 426 (2022) 127844.
- [38] Y.A. Akbas, S. Yusan, S. Sert, S. Aytas, Sorption of Ce(III) on magnetic/olive pomace nanocomposite: isotherm, kinetic and thermodynamic studies, *Environ. Sci. Pollut. Res.* 28 (2021) 56782–56794.
- [39] H. Yuhua, L. Xiaogang, S. Minxin, Q. Yuanyuan, L. Xiancai, Study on the adsorption of lanthanum ion imprinted on SBA-15/Y, *J. Indian Chem. Soc.* 99 (2022) 100425.
- [40] J. Gaete, L. Molina, F. Valenzuela, C. Basualto, Recovery of lanthanum, praseodymium and samarium by adsorption using magnetic nanoparticles functionalized with a phosphonic group, *Hydrometallurgy* 203 (2021) 105698.
- [41] E. Kusrinia, W. Wicaksono, C. Gunawan, N.Z.A. Daud, A. Usman, Kinetics, mechanism, and thermodynamics of lanthanum adsorption on pectin extracted from durian rind, *J. Environ. Chem. Eng.* 6 (2018) 6580–6588.
- [42] H. Javadian, M. Ruiz, M. Taghvai, A.M. Sastre, Novel magnetic nanocomposite of calcium alginate carrying poly (pyrimidine-thiophene-amide) as a novel green synthesized polyamide for adsorption study of neodymium, terbium, and dysprosium rare-earth ions, *Colloids Surf. A* 603 (2020) 125252.
- [43] M.M. Yusoff, N.R.N. Mostapa, M.S. Sarkar, T.K. Biswas, M.L. Rahman, S.E. Arshad, M.S. Sarjadi, A.D. Kulkarni, Synthesis of ion imprinted polymers for selective recognition and separation of rare earth metals, *J. Rare Earth* 35 (2017) 177–186.
- [44] Radwa M. Ashour, Ramy El-sayed, Ahmed F. Abdel-Magied, Ahmed A. Abdel-khalek, M.M. Ali, Kerstin Forsberg, A. Uheida, Mamoun Muhammed, Joydeep Dutta, Selective separation of rare earth ions from aqueous solution using functionalized magnetite nanoparticles: kinetic and thermodynamic studies, *Chem. Eng. J.* 327 (2017) 286–296.
- [45] G.S. dos Reis, G.L. Dotto, J. Vieillard, M.L.S. Oliveira, S.F. Lütke, L.F.O. Silva, E. C. Lima, N.P.G. Salau, U. Lassi, Uptake the rare earth elements Nd, Ce, and La by a commercial diatomite: kinetics, equilibrium, thermodynamic and adsorption mechanism, *J. Mol. Liq.* 389 (2023) 122862, <https://doi.org/10.1016/j.molliq.2023.122862>.
- [46] M. Medykowska, M. Wisniewska, K. Szewczuk-Karpisz, R. Panek, Interaction mechanism of heavy metal ions with the nanostructured zeolites surface – adsorption, electrokinetic and XPS studies, *J. Mol. Liq.* 357 (2022) 119144.
- [47] L.H. Dong, L.A. Hou, Z.S. Wang, P. Gu, G.Y. Chen, R.F. Jiang, A new function of spent activated carbon in BAC process: removing heavy metals by ion exchange mechanism, *J. Hazard. Mater.* 359 (2018) 76–84.
- [48] G.S. dos Reis, A. Grimm, D.A. Fungaro, T. Hu, I.A.S. de Brum, E.C. Lima, M. Naushad, G.L. Dotto, U. Lassi, Synthesis of sustainable mesoporous sulfur-doped biobased carbon with superior performance sodium diclofenac removal: Kinetic, equilibrium, thermodynamic and mechanism, *Environ. Res.* 251 (2024) 118595.
- [49] G.S. dos Reis, G.L. Dotto, J. Vieillard, M.L.S. Oliveira, S.F. Lutke, A. Grimm, L.F. O. Silva, E.C. Lima, M. Naushad, U. Lassi, Nickel-aluminium layered double hydroxide as an efficient adsorbent to selectively recover praseodymium and samarium from phosphogypsum leachate, *J. Alloy. Compd.* 960 (2023) 170530.